Available online at www.sciencedirect.com
SCIENCE DIRECT®
Journal of the European Ceramic Society 26 (2006) 149–160
www.elsevier.com/locate/jeurceramsoc

Particle shape and suspension rheology of short-fiber systems

Willi Pabst [a,*], Eva Gregorová [a], Christoph Berthold [b]

[a] *Department of Glass and Ceramics, Institute of Chemical Technology Prague, Technická 5, 166 28 Prague 6, Czech Republic*
[b] *Institut für Geowissenschaften, Arbeitsbereich Mineralogie und Geodynamik (Angewandte Mineralogie), Universität Tübingen, Wilhelmstrasse 56, 72074 Tübingen, Germany*

Received 1 July 2004; received in revised form 9 October 2004; accepted 16 October 2004
Available online 26 December 2004

Abstract

The effective viscosity of short-fiber suspensions is studied from a theoretical and experimental point of view. The theory of dilute suspensions with elongated particles is briefly summarized and explicit formulae for the dependence of the intrinsic viscosity on the particle shape (aspect ratio) are given in a form that should be useful for practical purposes. Concentration regimes, the influence of Brownian motion and sedimentation kinetics are mentioned. The effective viscosity of suspensions of two polydisperse wollastonites with significantly different average aspect ratios (approximately 5 and 16, respectively) is measured in dependence of the solids volume fraction and fitted with power-law models (Krieger and Maron–Pierce relations). It is shown that the intrinsic viscosity determined is higher than theoretically predicted via the Brenner formula, while the critical volume fraction is lower than predicted by the empirical Kitano relation. Possible reasons for these discrepancies, common to most real polydisperse systems, are discussed.

Keywords: Rheology; Suspensions; Fibers; Whiskers; Silicates; Wollastonite

1. Introduction

Particles with anisometric shape are ubiquitous in ceramic technology and materials processing, in general. When properly oriented (e.g. by flow processes) materials with more or less anisotropic microstructures can be prepared. In particular, elongated particles (e.g. short fibers or whiskers) can be used to increase the strength and fracture toughness of composites (e.g. ceramic matrix composites). In the case of (a certain degree of) preferred orientation (e.g. flow-induced), short-fiber composites are transversally isotropic materials. Therefore, the study of the rheology of fiber suspensions, in particular, their effective viscosity and its concentration dependence, is of general interest in ceramic technology and technology today. There is, however, a paradoxical situation with respect to fiber suspensions: a considerable amount of theoretical work has been done during the 20th century (including extensive work on the relationship between particle shape and rheology) but most serious results are still hidden in the original literature and have not yet found their way into monographs and textbooks. Therefore, many of the results achieved by theoreticians in the field are not easily accessible to the majority of skillful experimenters. In this paper, we propose, using two wollastonite systems as paradigmatic examples, a systematic way to confront well-founded theoretical results with results of experimental measurements on real systems. In particular, we give a very simple relation for the dependence of the intrinsic viscosity on aspect ratio (Eq. (35)), which approximates the highly sophisticated Brenner relation (Eq. (17)) for many practical situations with sufficient precision. We assume that this approximate relation, formally the "non-Brownian" counterpart of the widely used Kuhn–Kuhn relation for low-aspect-ratio Brownian particles (Eq. (31)), will be appealing to other experimental investigators.

Wollastonite, the material chosen as a paradigmatic example for the present study, is an inosilicate (single-chain sili-

* Corresponding author.
E-mail address: pabstw@vscht.cz (W. Pabst).

0955-2219/$ – see front matter © 2004 Elsevier Ltd. All rights reserved.
doi:10.1016/j.jeurceramsoc.2004.10.016

cate, $CaSiO_3$). As a result of the internal structure and preferred cleavage along the directions [1 0 0] and [0 0 1], the usual external shape of wollastonite particles is that of elongated needles. According to the recent literature,[1] the experimentally measured density of both triclinic and monoclinic wollastonite is between 2.86 and 3.09 g/cm^3, although the calculated theoretical value is around 2.90 g/cm^3 for both and the JCPDS data sheets[2] list values of 2.91–2.92 g/cm^3. Due to its elongated, needle-like shape wollastonite can be used in ceramic technology to increase the green strength of as-dried ceramic products, which need further manipulation in a production line. This can be especially advantageous for large ceramic parts in those cases where a certain CaO content can be tolerated in the raw material mixture (e.g. in sanitary ware production). Elongated particles, however, lead to an increase in the viscosity of ceramic suspensions that exceeds the usual increase encountered for isometric particles. This is usually a disadvantage in ceramic processing, although in other areas of application this large viscosity-increasing effect of elongated particles might be used to achieve high viscosities with relatively low solids loadings (volume fractions).

The practical objective of this work is two-fold: first, to characterize the viscosity increase with volume fraction for polydisperse wollastonite suspensions containing particles with different average shape (average aspect ratio). Second, to compare the measured results with existing theoretical models and empirical relations and discuss the applicability of the latter for prediction purposes.

Section 2 introduces the basic quantities (effective, relative and intrinsic viscosity) and briefly summarizes the theory of dilute suspensions with elongated particles. Explicit formulae for the dependence of the intrinsic viscosity on the particle shape (aspect ratio) are given in a form that should be useful in practice. Concentration regimes, the influence of Brownian motion and sedimentation kinetics are also discussed for the case of suspensions with elongated particles (fiber suspensions). Section 3 gives material characteristics and experimental details concerning the wollastonite suspensions investigated in this work. Section 4 presents measured data and evaluated results, including the fit parameters determined. Results obtained on the basis of experimentally measured data are discussed and compared to the predictions.

2. Theoretical

2.1. Effective, relative and intrinsic viscosity

Effective properties are the macroscopic (i.e. overall or large-scale), properties of multiphase materials. In general, they are dependent on the constituent (i.e. phase) properties and the microstructure of the material. For two-phase solid–liquid mixtures with matrix-inclusion type microstructure (suspensions), an effective shear viscosity η (simply called "effective viscosity" in the sequel) can be defined and assumed to be a function of the solids volume fraction ϕ. Note, however, that the assumption of a dependence exclusively on ϕ is only justifiable on pragmatic grounds, i.e. when higher-order microstructural information is lacking (cf. the discussions in[3,4] and the references given therein). Note further, that in assuming the existence of a unique (i.e. not shear rate-dependent) shear viscosity, one implicitly assumes purely viscous behavior (i.e. no viscoelastic effects) and Newtonian (linear) behavior of the whole suspension (and not only of the suspending medium). In the dilute limit, i.e. for volume fractions $\phi \to 0$, the effective viscosity η of suspensions with rigid, spherical particles is usually assumed to obey the Einstein relation[5]

$$\eta = \eta_0(1 + 2.5\phi). \tag{1}$$

In this equation, ϕ is the solids volume fraction, η denotes the effective suspension viscosity and η_0 the viscosity of the suspending medium (pure liquid). In order to simplify notation in the following text, we introduce the relative viscosity η_r

$$\eta_r \equiv \frac{\eta}{\eta_0}, \tag{2}$$

and the so-called intrinsic viscosity $[\eta]$

$$[\eta] \equiv \lim_{\phi \to 0} \frac{\eta_r - 1}{\phi}. \tag{3}$$

Using the intrinsic viscosity, the Einstein relation can be formally generalized to suspensions of anisometric particles, i.e.

$$\eta_r = 1 + [\eta]\phi. \tag{4}$$

Jeffery, in a rigorous treatment of the motion of a rigid ellipsoids and spheroids with a certain aspect ratio,[6] was the first to calculate values for $[\eta]$ as a function of the particle aspect ratio. Therefore, we call Eq. (4) the Jeffery–Einstein relation.

At this point, it should be emphasized that Einstein's value of 2.5 for the intrinsic viscosity of dilute sphere suspensions, though widely assumed to be valid, is not universally acknowledged and has been questioned from the theoretical as well as from the experimental side. Mention should be made of Happel's alternative theoretical result[7,8]

$$\eta = \eta_0(1 + 5.5\phi), \tag{5}$$

and of the so-called Bačinskij relation[9–11]

$$\eta = \eta_0(1 + 4.5\phi), \tag{6}$$

probably based on empirical findings. Unfortunately, the original Russian source of this relation could not be identified (ante 1952). It occurs, however, in some of the older Czech literature[9,10] and is reported to be more appropriate than the Einstein relation (1). Note that both Eqs. (5) and (6) are meant for spherical or isometric particles. Thus, the deviation of the intrinsic viscosity $[\eta]$ from Einstein's value 2.5 in these two relations has nothing to do with anisometric particle shape.

2.2. Model shapes and concentration regimes for suspensions of elongated particles

Isometric particles have approximately the same size in all directions. Apart from the ideal case of spheres, isometric are, e.g. all regular polyhedra (tetrahedra, cubes, octahedra, dodecahedra and icosahedra) and many other facetted and irregular particles. Anisometric particles have at least one distinguished direction along which their size is significantly larger or smaller than perpendicular to it. The simplest model shapes for approximating real anisometric particles are rotational ellipsoids (i.e. prolate and oblate spheroids) and circular cylinders (i.e. rods and discs or fibers and platelets). In both cases shape can be quantified via a single number, the aspect ratio. It is evident that the first is the most natural from a principal point of view, because it includes the sphere as a special case. Moreover, only for spheroids the hydrodynamic problem of particle motion in a viscous fluid can be solved exactly. This is the reason why spheroids are the preferred model shapes, e.g. in the rheology of fiber and platelet suspensions.[12–16] Defining the aspect ratio R as the ratio between the long and short axes or half-axes (height/diameter ratio in the case of cylinders), one can distinguish prolate (elongated) particles with $R > 1$ and oblate (flaky) particles with $R < 1$.

Of course, for real particle systems (powders), which are usually polydisperse with respect to size and shape, the determination of the aspect ratio is not an easy task and need not even be useful in all cases, since shape (quantified via the aspect ratio) need not be (and in general is not) size-invariant. In other words, similar to the size, also the shape (aspect ratio) exhibits a distribution, e.g. in the case of oblate particles (discs) certain shape information, related to the aspect ratio, can be extracted from the comparison of sedimentation and laser diffraction data,[17–21] but the interpretation of these results is principally complicated by the fact that, in addition to the size distribution, there is a superimposed shape distribution in a real particle system. Nevertheless, in certain cases (viz. when the shape distribution is not correlated to the size distribution, i.e. for each size class the shape distribution is approximately the same), an average aspect ratio $\overline{R}$ (usually the arithmetic mean of individual aspect ratios or of partial size class averages) can be calculated for the system as a whole.[22,23]

For suspensions with elongated particles (modeled as long prolate spheroids or long slender rods), in the following simply called “fiber suspensions”, it is useful to distinguish three concentration regimes: dilute, semi-dilute and concentrated.[13,14,24–26] According to the Doi–Edwards model for monodisperse fiber suspensions,[24,25] the dilute regime should be characterized by the condition

$$\phi < \frac{1}{R^2}, \tag{7}$$

which is derived from the condition that the mean distance between fibers is larger than half of the fiber length, i.e. the fiber can freely rotate in arbitrary directions. According to some authors,[26,27] this estimate is too strictly limiting. Instead of the volume fraction occurring in Eq. (7), they propose a value larger by a factor of 24 for the transition from dilute to semi-dilute. In the semi-dilute regime (where the particles are not free to rotate end-over-end, but are still sufficiently far apart for the mutual hydrodynamic drag exerted by neighboring particles to be small), it is necessary to distinguish the case of randomly oriented fibers, for which

$$\frac{1}{R^2} < \phi < \frac{1}{R}, \tag{8}$$

and the case of preferentially oriented (aligned) fibers, for which

$$\frac{1}{R^2} < \phi < 1. \tag{9}$$

In the theory of fiber suspensions the isotropic concentrated regime (where the fiber orientation is random) is defined by the condition[13,14,25]

$$\frac{1}{R} < \phi, \tag{10}$$

while the maximum concentration up to which the suspensions can remain isotropic is (according to the Onsager theory)[26]

$$\phi < \frac{3.3}{R}. \tag{11}$$

Higher concentrations can only be achieved when isotropy is abandoned (nematic state). Table 1 lists the concentration regimes for monodisperse (with respect to size and shape) particle systems according to Eqs. (7), (10) and (11) in dependence of the particle aspect ratio R. Evidently, Eq. (10) cannot apply to isometric particles, and Eqs. (10) and (11) are useless for this case. For a suspension of monodisperse spheres, e.g. the critical volume fraction ϕ_c is approximately 64% (cf.[4,28–30]). This value (much lower than 100%, as predicted by Eqs. (7) and (10)) cannot be exceeded unless the suspension looses its ability to flow (blocking phenomenon). For such a system, volume fractions higher than approximately 52% (corresponding to primitive cubic packing) should certainly be considered as being in the concentrated regime, since the particles are in direct steric contact (excluded-volume interactions). The densest packing of monodisperse spheres (hexagonal closest packing (hcp) or face-centered cubic (fcc)) corresponds to a volume fraction of approximately 74%, while the mentioned approximate value of 64% corresponds to random close packing (rcp). In the case of monodisperse fibers, the densest packing can be as high as 91%, but usually no estimates of the lower bound can be given. In the case of real systems, which are usually polydisperse, the critical volume fraction has to be determined empirically.

Table 1
Concentration regimes (volume fraction limits in %) of monodisperse (with respect to size and shape) fiber suspensions in dependence of the aspect ratio, according to Eqs. (7), (10) and (11)

Aspect ratio (R)	Dilute for $\phi < 1/R^2$	Transition from semi-dilute to isotropic concentrated at $\phi < 1/R$	Maximum concentration of isotropic suspensions at $\phi < 3.3/R$
1	100	100	(330)
2	25	50	(165)
3	11	33.3	(110)
4	6.25	25	82.5
5	4	20	66
10	1	10	33
16	0.39	6.25	20.6
25	0.16	4	13.2
50	0.04	2	6.6
100	0.01	1	3.3
1000	0.0001	0.1	0.33
1000000	10^{-10}	0.0001	0.00033

2.3. Dependence of the relative viscosity on the solids volume fraction

In a first approximation (cf. the discussion earlier), the relative viscosity of a suspension η_r can be assumed to be a function of the solids volume fraction ϕ, i.e.

$$\eta_r = \eta_r(\phi). \tag{12}$$

There have been numerous attempts to find expressions that extending the validity of the Jeffery–Einstein relation (Eq. (4)) to non-dilute systems (cf.[4] and the references cited therein). Both exponential (Mooney-type) and power-law (Krieger-type) relations are popular, although the latter exhibit a subtle advantage from the theoretical point of view.[4] The Krieger relation[31] is

$$\eta_r = \left(1 - \frac{\phi}{\phi_c}\right)^{-[\eta]\phi_c}. \tag{13}$$

As the case may be, this relation can be considered as a model equation for the prediction of the effective viscosity of suspensions with monodisperse spheres (in this case set $[\eta] = 2.5$ and $\phi = 0.64$) or as a fit equation with one (ϕ_c) or two (ϕ_c and $[\eta]$) adjustable fit parameters. Note that the Krieger relation exhibits correct limit behavior, i.e. the relative viscosity relation reduces to the Jeffery–Einstein relation (Eq. (4)) for $\phi \to 0$ and goes to infinity, $\eta_r \to \infty$, as the volume fraction approaches $\phi \to \phi_c$, as required.

Another useful relation is the Maron–Pierce relation[32]

$$\eta_r = \left(1 - \frac{\phi}{\phi_c}\right)^{-2}, \tag{14}$$

which can be considered as a special case of the Krieger relation, obtained by setting $[\eta]\phi_c = 2$. The Maron–Pierce relation can be used for fitting purposes instead of the Krieger relation when a two-parameter fit is to be avoided but the intrinsic viscosity $[\eta]$ is not known. It is widely used and recommended in the literature on fiber suspensions.[22,33–35] It seems that the reason for the success of the Maron–Pierce relation in practice is to be sought in the fact that for monodisperse spheres $[\eta]\phi \approx 1.85$ which is for practical purposes sufficiently close to the Maron–Pierce value of 2. With growing particle anisometry, on the other hand, the expected decrease in the critical volume fraction ϕ_c is in part compensated by an increase in the intrinsic viscosity $[\eta]$. With respect to this fact, the value $2/\phi_c$ determined from fitting with the Maron–Pierce relation (Eq. (14)), can be considered as a rough estimate for the intrinsic viscosity $[\eta]_{est}$.

Kitano et al.[22] used the Maron–Pierce relation for data fitting. Based on experiments with polymer melts containing different volume fractions of fibers with different average aspect ratio $\bar{R}$ (ranging from 6 to 27), they found an approximately linear relation between ϕ_c and the average aspect ratio $\bar{R}$

$$\phi_c = 0.54 - 0.0125\bar{R}, \tag{15}$$

sometimes reported with other coefficients, viz. $\phi_c = 0.53 - 0.013\bar{R}$ (cf.[33,34]). Although Eq. (15) is often used and sometimes recommended for prediction purposes, when a rough estimate of the effective viscosity of fiber suspensions is required and an alternative is not in sight, it has to be kept in mind that it is a purely empirical finding. In particular, the numerical values can be subject to change.

2.4. Dependence of the intrinsic viscosity on the particle aspect ratio

The intrinsic viscosity is a parameter characterizing the behavior of non-interacting particles in a dilute suspension. Thus, it is rather a characteristic of the particle system than of the suspension as a whole. From this, it is plausible that the intrinsic viscosity depends in the first instance on particle shape, i.e. the particle aspect ratio R

$$[\eta] = [\eta](R). \tag{16}$$

Note that the intrinsic viscosity is in general bounded from below by the inequality[12,36]

$$[\eta] > 1.$$

According to Brenner,[12] the intrinsic viscosity for simple shear flow of a suspension with axisymmetric particles (possessing fore-aft symmetry) is given by the expression

$$[\eta] = 5Q_1 - \frac{15}{4}Q_2\langle\sin^2\theta\rangle - \frac{5}{4\mathrm{B}}(3Q_2 + 4Q_4) \times \langle\sin^2\theta\,\cos 2\phi\rangle + \frac{15}{2\mathrm{BP}}(3Q_2 + 4Q_3)\langle\sin^2\theta\,\sin 2\phi\rangle. \tag{17}$$

In this expression

$$B = \frac{5N}{3K_\mathrm{r}} \tag{18}$$

is a dimensionless parameter and

$$P = \frac{\gamma}{D_\mathrm{r}} \tag{19}$$

is the rotary Péclet number, with γ being the shear rate and the rotary Brownian diffusion coefficient D_r given by the Stokes–Einstein equation[37]

$$D_\mathrm{r} = \frac{kT}{6V\eta_0 K_\mathrm{r}}, \tag{20}$$

where k is the Boltzmann constant, T the absolute temperature, V the particle volume and η_0 the viscosity of the suspending medium. The material constants N and K_r (connected to the rotation of the axisymmetric particle about a transverse axis) are dependent on the model shape chosen and the aspect ratio (true axis ratio, particle axis ratio) $R = a/b$, where a is the polar radius (for prolate shapes half of the length, for oblate shapes half of the thickness) and b the equatorial radius (for prolate shapes half of the thickness, for oblate shapes half of the diameter). For spheroids, in general,

$$K_\mathrm{r} = \frac{2(R^2+1)}{3(R^2\alpha_1 + \alpha_2)}, \tag{21}$$

and

$$N = \frac{2(R^2-1)}{5(R^2\alpha_1 + \alpha_2)}. \tag{22}$$

Moreover,

$$Q_1 = \frac{1}{5\alpha_3}, \tag{23a}$$

$$Q_2 = \frac{2}{15\alpha_3}\left(1 - \frac{\alpha_5}{\alpha_6}\right), \tag{23b}$$

$$Q_3 = \frac{1}{5\alpha_3}\left[\frac{R(\alpha_1+\alpha_2)}{R^2\alpha_1+\alpha_2}\left(\frac{\alpha_3}{\alpha_4}\right) - 1\right], \tag{23c}$$

and

$$Q_4 = \frac{1}{5\alpha_3}\left[\frac{2R\alpha_3}{(R^2+1)\alpha_4} - 1\right]. \tag{23d}$$

In these expressions, the α's are defined as

$$\alpha_1 = \frac{2}{R^2-1}(\beta R^2 - 1), \tag{24a}$$

$$\alpha_2 = \frac{R^2}{R^2-1}(1-\beta), \tag{24b}$$

$$\alpha_3 = \frac{R^2}{4(R^2-1)^2}(3\beta + 2R^2 - 5), \tag{24c}$$

$$\alpha_4 = \frac{R}{(R^2-1)^2}(R^2 + 2 - 3\beta R^2), \tag{24d}$$

$$\alpha_5 = \frac{R^2}{4(R^2-1)^2}(2R^2 + 1 - (4R^2-1)\beta), \tag{24e}$$

$$\alpha_6 = \frac{R^2}{(R^2-1)^2}[(2R^2+1)\beta - 3], \tag{24f}$$

where

$$\beta = \frac{\operatorname{arccosh} R}{R\sqrt{R^2-1}}, \tag{25}$$

for prolate spheroids ($R > 1$). As a consequence,

$$B = \frac{R^2-1}{R^2+1}. \tag{26}$$

The volume of a prolate spheroid is

$$V = \frac{4\pi}{3}ab^2 = \frac{4\pi}{3}Rb^3. \tag{27}$$

For prolate spheroids, like for all axisymmetric particles with fore-aft symmetry, the material parameters Q_1 through Q_4, together with K_r, N, and B completely determine the behavior of the suspension in arbitrary flow processes.[12] Only five of these parameters are independent and all material parameters are uniquely defined by the aspect ratio R. Based on the knowledge of K_r and the particle size (volume V), the rotary Péclet number can be estimated, cf. Eq. (19), in order to assess the influence of Brownian motion. It is common practice to distinguish three regimes:[12]

- Dominant Brownian motion:

  $$P \ll 1. \tag{28}$$

  In this case ("zero shear rate limit"), the intrinsic viscosity $[\eta]_0$ is maximal and can be considered as an upper bound of the intrinsic viscosity. Eq. (17) can be approximated as

  $$[\eta]_0 = 5Q_1 - Q_2 + 2Q_3. \tag{29}$$

  For high-aspect-ratio spheroids ($R \gg 1$), this equation reduces to the well-known approximate result of Kuhn and

Table 2
Upper bound of the intrinsic viscosity $[\eta]_0$ ($P = 0$), calculated according to Eq. (29), and lower bound of the intrinsic viscosity $[\eta]_\infty$ ($P \to \infty$), calculated according to Eq. (17), for dilute suspensions of prolate spheroids in dependence of the aspect ratio[12]

R	$[\eta]_0$	$[\eta]_\infty$
1	2.5	2.5
2	2.91	2.57
3	3.68	2.68
4	4.66	2.8
5	5.81	2.92
6	7.1	3.06
7	8.53	3.14
8	10.1	3.27
9	11.8	3.38
10	13.6	3.44
12	17.7	3.69
14	22.2	3.88
16	27.2	3.93
18	32.6	4.17
20	38.5	4.37
50	176.8	7.68
100	593.7	20.4

First three values in the third column (for R between 1 and 3) corrected according to Scheraga's exact numerical calculation.[40]

Kuhn[38]

$$[\eta]_0 = \frac{R^2}{15}\left[\frac{3}{\ln 2R - 0.5} + \frac{1}{\ln 2R - 1.5}\right] + \frac{8}{5}, \tag{30}$$

while for low-aspect-ratio spheroids ($R < 15$), the approximate expression

$$[\eta]_0 = 2.5 + 0.408(R-1)^{1.508}, \tag{31}$$

can be used.[13] The second column in Table 2 lists this upper bound of the intrinsic viscosity $[\eta]_0$ (i.e. in the case, $P = 0$), calculated according to Eq. (29), for dilute suspensions of prolate spheroids in dependence of the aspect ratio.[12]

- Intermediate Brownian motion:

$$R^3 + R^{-3} \gg P \gg 1. \tag{32}$$

Although in this case the goniometric factors in Eq. (17) adopt very simple expressions,[39] an explicit calculation of the intrinsic viscosity in the intermediate regime is rather intricate.[12] However, since intermediate Brownian motion necessarily requires very large aspect ratios ($R \gg 1$) for prolate spheroids, the approximation[12]

$$[\eta]_i = 2 + \lambda\frac{R^2}{\ln R}P^{-1/3}, \tag{33}$$

valid for long thin prolate spheroids (with λ between 0.2 and 0.5), might be a used as an estimate in this region.

- Weak Brownian motion:

$$P \gg 1 \quad \text{and} \quad P \gg R^3 + R^{-3}. \tag{34}$$

In this case, the goniometric factors to be inserted in Eq. (17) are given in Table 3 in dependence of the aspect ratio, according to Brenner,[12] based on the asymptotic results of Hinch and Leal.[39] The third column in Table 2 lists the lower bound of the intrinsic viscosity $[\eta]_\infty$ (i.e. in the case $P \to \infty$), calculated according to Eq. (17), for dilute suspensions of prolate spheroids in dependence of the aspect ratio. The first three values (for R between 1 and 3) have been corrected according to Scheraga's exact numerical calculation.[40] For aspect ratios between $R = 1$ and approximately $R = 50$, the following expression can be used

$$[\eta]_\infty = 2.5 + 0.123(R-1)^{0.925}. \tag{35}$$

This simple expression is in formal agreement with Eq. (31) and has been obtained by fitting the $[\eta]_\infty$ values in Table 2 in the aspect ratio range from $R = 1$ to $R = 20$ (with correlation coefficient 0.998).

Table 3
Goniometric factors to be inserted in Eq. (17) in dependence of the aspect ratio, according to Brenner,[12] based on the results of Hinch and Leal[39]

R	$\langle \sin^2\theta \rangle$	$P\langle \sin^2\theta \sin^2\phi \rangle$	$\langle \sin^2\theta \sin^2\phi \rangle$
1	0.667	0	0
2	0.690	2.1653	−0.2716
3	0.727	4.9557	−0.4886
4	0.758	8.6551	−0.5136
5	0.784	13.302	−0.5810
6*	0.804	19.395	−0.6264
7	0.823	25.487	−0.6718
8*	0.836	27.929	−0.6989
9*	0.849	36.464	−0.7259
10	0.862	51.090	−0.7530
12*	0.876	77.033	−0.7809
14*	0.891	102.98	−0.8087
16	0.905	128.92	−0.8366
18*	0.912	169.73	−0.8489
20*	0.919	210.53	−0.8611
50	0.968	1244.68	−0.9388
100	0.986	4998.81	−0.9578

The asterisk denotes interpolated values.

Brenner's analysis,[12] on which the above summary is essentially based, is probably the most comprehensive, most precise and most widely acknowledged theoretical investigation in this field. However, when practical applications of these results are intended, a general note of warning might be in place. In particular, the attempt to correlate particle shape (aspect ratio) with suspension rheology (intrinsic viscosity) is principally complicated by two facts:

First, the intrinsic viscosity value determined as a fit parameter via the Krieger relation (13) (or, the estimate for it obtained via the Maron–Pierce relation (14)) from experimentally measured relative suspension viscosities is necessarily subject to statistical and systematic errors. Statistical errors may result from imperfect measurement precision (instrumental errors, errors due to sedimentation during viscosity measurement and concentration errors due to imperfect sample preparation) and the sensitivity of the non-linear regression fits to small changes in the data. Systematic errors result from the fact that the measurements are necessarily performed in the non-dilute range, where interactions play

a non-negligible role. A correct value for the intrinsic viscosity can be expected only for perfectly deagglomerated (homogeneous) and stable (uniform, i.e. non-sedimentating) suspensions. Only in such a case, the intrinsic viscosity value obtained from the Krieger fit (Eq. (13)) corresponds to the Jeffery–Einstein coefficient $[\eta]$ in Eq. (4). As long as attractive particle interactions cannot be completely excluded, however, i.e. as long as there is an albeit small tendency of agglomeration, the intrinsic viscosity value determined from experimental measurements, must necessarily be higher than theoretically predicted, because the tangent slope at $\phi = 0$ is exaggerated. Brenner[12] reports, e.g. that in the case of doublets in the form of (two) touching spheres the upper and lower limit of the intrinsic viscosity of the doublet suspension is $[\eta]_0 = 3.58$ and $[\eta]_\infty = 3.02$, respectively, in contrast to the Einstein value of $[\eta] = 2.5$ for spheres.

Second, it has to be kept in mind that the theoretical expressions derived for the $[\eta](R)$ dependence hold for a particle system with a unique aspect ratio, i.e. all particles, whatever their size, are assumed to have the same (in mathematical terms "similar") shape. For a particle system with a range of aspect ratios, it is in fact not clear a priori, what (if any) is the appropriate average aspect ratio to be inserted in the theoretically derived intrinsic viscosity formulae. Naturally, in lack of a better-justified alternative, it is reasonable to assume the arithmetic mean of the individual aspect ratios as a useful average value.[22,23]

3. Experimental

3.1. Material characterization

For the preparation of suspensions, two commercially available types of wollastonite were used, WM 45 (supplied by Franz Mandt GmbH, Wunsiedel, Germany) and HSV 45 (supplied by Osthoff-Petrasch GmbH, Norderstedt, Germany). According to the respective suppliers both exhibit a subsieve size below 45 μm. A detailed size and shape characterization of these two wollastonite types, including a comparison of laser diffraction and image analysis results, has been given elsewhere.[23] An earlier laser diffraction study with the wollastonite type HSV 45 demonstrated the effect of particle orientation in the flow-through cell of laser instruments on the interference pattern.[41] It has been shown that the interference pattern of this type of wollastonite is highly non-circular when the particles are aligned in the flow direction.[41] According to laser diffraction (Analysette 22, Fritsch GmbH, Idar-Oberstein, Germany), only 77 and 60 vol.% for WM 45 and HSV 45, respectively, are <45 μm. Table 4 lists the size characteristics[23] determined by laser diffraction and by microscopic image analysis (Lucia G, Laboratory Imaging s.r.o., Prague, Czech Republic).

The average aspect ratio determined by image analysis[23] is approximately 5 and 16 for WM 45 and HSV 45, respectively, with a large statistical scatter in both cases (relative standard deviation approximately 50%). The density, measured by helium pycnometry (AccuPyc 1330, Micrometritics, Norcross, USA), was 2.90 ± 0.01 g/cm^3 for both types of wollastonite powder.

Table 4
Size characteristics (median values of volume-weighted cumulative curves) of wollastonite types WM 45 and HSV 45

Size measure	WM 45	HSV 45
D_{F-} (median)	20.6	29.9
D_P (median)	45	98
D_{F+} (median)	103	432
D_L (median)	21.6	29.1

D_P, projected area diameter; D_L, laser diffraction equivalent diameter; D_{F-} and D_{F+}, minimum and maximum Feret diameter, respectively.

Starch suspensions were prepared for reasons of comparison. Two starch types were applied, corn starch (Gustin, Dr. Oetker s.r.o., Kladno, Czech Republic) and wheat starch (unspecified, Amylon a.s., Havličkův Brod, Czech Republic). The shape of the starch globules is close to spherical, i.e. the average aspect ratio approximately 1. The median size (laser diffraction) is 14.2 and 20.0 μm, respectively, the density approximately 1.45 g/cm^3.

3.2. Experimental details

Effective suspension viscosities were measured at room temperature ($T = 25.5 \pm 0.9$ °C). In order to slow down sedimentation, a 60 wt.% sugar (saccharose) solution was used as the suspending medium instead of water. According to the literature,[42] the density of this sugar solution at this temperature is $\rho = 1.284 \pm 0.001$ g/cm^3, its viscosity $\eta_0 = 42.8 \pm 2.3$ mPa s (cf. Table 5). The density of our sugar solution was densimetrically (using a plunger) measured to be $\rho = 1.285$ g/cm^3, the viscosity values measured by rotational

Table 5
Density and viscosity of a 60 wt.% sugar solution as a function of temperature

T (°C)	ρ (g/cm^3)	η_0 (mPa s)
20	1.2865	58.5
20.5		56.8
21	1.2860	55.2
21.5		53.6
22	1.2855	52.1
22.5		50.6
23	1.2850	49.2
23.5		47.8
24	1.2845	46.5
24.5		45.2
25	1.2840	44.0
25.5		42.8
26	1.2835	41.7
26.5		40.6
27	1.2830	39.5
27.5		38.4
28	1.2825	37.4
28.5		36.5
29	1.2820	35.5
29.5		34.6
30	1.2815	33.7

viscometry (RotoVisco 1 with coaxial cylinder system Z 41, ThermoHaake, Karlsruhe, Germany) exhibited an average of approximately 43 mPa s.

Due to the higher density and viscosity of the sugar solutions sedimentation times are increased by a factor of approximately 50 in the case of wollastonite and by a factor of approximately 120 in the case of starch. Suspensions of different concentrations (solids volume fractions) were prepared by mixing, shaking (1200 s, laboratory shaker HS 206 B, IKA Werke, Staufen, Germany) and ultrasonication (60 s, ultrasonic processor UP 200S with probe S14, Dr. Hielscher GmbH, Stuttgart, Germany). Viscosities were measured at a shear rate of 1000 s^{-1}. The measuring schedule was 60 s ramp up, 30 s hold at 1000 s^{-1} and 60 s ramp down. For the concentrations presented in the next section, all flow curves were linear (i.e. indicative of Newtonian behavior) and without hysteresis (i.e. sedimentation during the measurement was negligible).

4. Results and discussion

In order to assess the influence of Brownian motion, we calculate the rotary Péclet number according to Eq. (19) for a shear rate of 1000 s^{-1}. In order to be on the safe side, we calculate the rotary Brownian diffusion coefficient according to Eq. (20) by assuming a minimum Feret diameter b of 10 μm in the particle volume formula (Eq. (27)). The resulting Péclet numbers at room temperature ($T = 25\,^{\circ}C$) are $P = 6.2 \times 10^9$ and 12.4×10^9 for WM 45 and HSV 45, respectively, which clearly corresponds to the case of weak Brownian motion. The theoretically predicted intrinsic viscosities [η] for this case are approximately 2.5, 2.8–2.9 and 3.9–4.0 for starch ($\bar{R} \approx 1$), WM 45 ($\bar{R} \approx 5$) and HSV 45 ($\bar{R} \approx 16$), respectively (cf. Table 2 and Eq. (35)). Using the empirical expression proposed by Kitano et al.[22] (Eq. (15)), we would predict critical volume fractions ϕ_c of 52.8, 47.8 and 34.0% for starch, WM 45 and HSV 45, respectively.

Tables 6 and 7 list the measured relative viscosities η_r for the two types of starch suspensions (corn and wheat) and the two types of wollastonite suspensions. The estimated relative errors are 3–4% for the starch suspensions and 15–17% for the wollastonite suspensions. Suspensions of HSV 45 with volume fractions >12 vol.% and of WM 45 with volume fractions >24 vol.% could not be measured in the viscometer (due to blocking and apparent wall slip phenomena, the flow curve exhibits a steep non-linear uprise followed by unpredictable fluctuations, not to be confused with true shear-thickening behavior, which must be excluded on theoretical grounds). In contrast, starch suspensions were measurable up to concentrations of approximately 30 vol.%. According to the Doi–Edwards classification of concentrational regimes (cf. Eqs. (7)–(11) and Table 1), WM 45 and HSV 45 suspensions can be considered as dilute only when the solids volume fraction is <4 and 0.4 vol.% (!), respectively. In terms of this classification scheme, WM 45 and HSV 45 suspensions with solids volume fractions >20 and >6.25 vol.%, respectively, have to be considered as concentrated.

Table 6
Relative viscosities η_r of starch suspensions in dependence of the starch volume fraction (starch density $\rho = 1.45\,g/cm^3$)

Volume fraction (%)	Corn starch	Wheat starch	Average of both starch types
1	0.97 ± 0.05	1.03	1.00 ± 0.03
2	1.02 ± 0.07	0.99 ± 0.05	1.01 ± 0.02
3	1.07 ± 0.03	1.12 ± 0.01	1.10 ± 0.03
5	1.18 ± 0.05	1.17 ± 0.07	1.18 ± 0.01
7	1.37 ± 0.03	1.35 ± 0.06	1.36 ± 0.01
10	1.66 ± 0.04	1.72 ± 0.01	1.69 ± 0.03
15	2.44 ± 0.16	2.21 ± 0.04	2.33 ± 0.12
20	2.82 ± 0.20	3.30 ± 0.09	3.06 ± 0.24
25	4.21 ± 0.10	4.58 ± 0.08	4.40 ± 0.19
30	Not measured	7.14	7.14
Average relative error (%)	4.4	2.9	3.2

Figs. 1–3 show the measured relative viscosities η_r, together with error bars (for the wollastonite suspensions) and the fit curves obtained by non-linear regression via Eqs. (13) (Krieger fit, dashed lines) and (14) (Maron–Pierce fit, full lines). The vertical asymptotics indicate the corresponding critical volume fractions ϕ_c obtained by fitting. Since the data series of both starch suspensions are sufficiently close to each other (as expected), average values have been used for fitting in this case.

Tables 8 and 9 list the values of the fit parameters [η] and ϕ_c, together with the correlation coefficients C as a measure of the quality of the fit, determined using the Krieger

Table 7
Relative viscosities η_r of wollastonite suspensions in dependence of the wollastonite volume fraction (wollastonite density $\rho = 2.9\,g/cm^3$)

Volume fraction (%)	WM 45	HSV 45
1	1.00 ± 0.16	
2	1.00 ± 0.10	1.0
3	1.03 ± 0.20	
4		1.1
5	1.18 ± 0.23	
6		1.27 ± 0.22
7	1.42 ± 0.19	
8		1.99 ± 0.30
9		2.48 ± 0.42
10	1.55 ± 0.21	3.04 ± 0.51
11		16.0
12	1.76 ± 0.23	30.6
14	1.85 ± 0.27	Not measurable
16	2.53 ± 0.33	
18	3.41 ± 0.51	
20	4.25 ± 0.65	
22	5.07 ± 0.73	
24	6.14 ± 0.89	
26	Not measurable	
Average relative error (%)	15	17

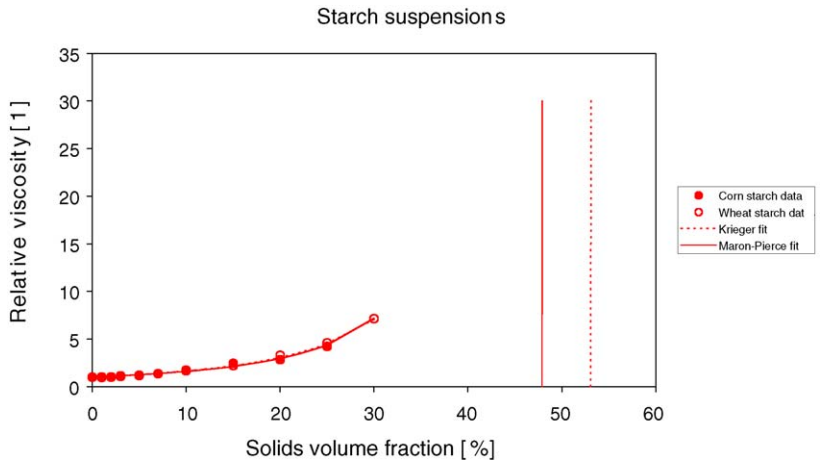

Fig. 1. Concentration dependence of the relative viscosity of starch suspensions (filled circles: corn starch; empty circles: wheat starch); dashed line: Krieger fit; full line: Maron–Pierce fit (the corresponding critical volume fractions ϕ_c obtained by fitting are indicated as vertical asymptotics).

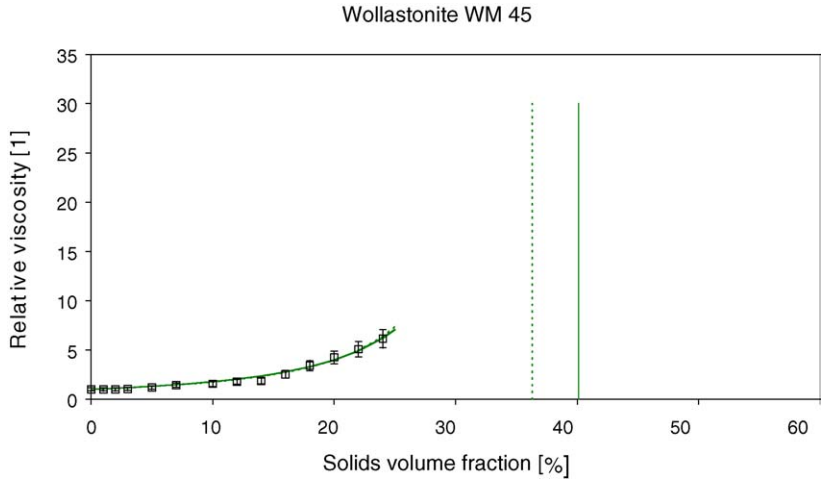

Fig. 2. Concentration dependence of the relative viscosity of suspensions with wollastonite WM 45; measured data (empty squares), Krieger fit (dashed line), Maron–Pierce fit (full line); the corresponding critical volume fractions ϕ_c obtained by fitting are indicated as vertical asymptotics.

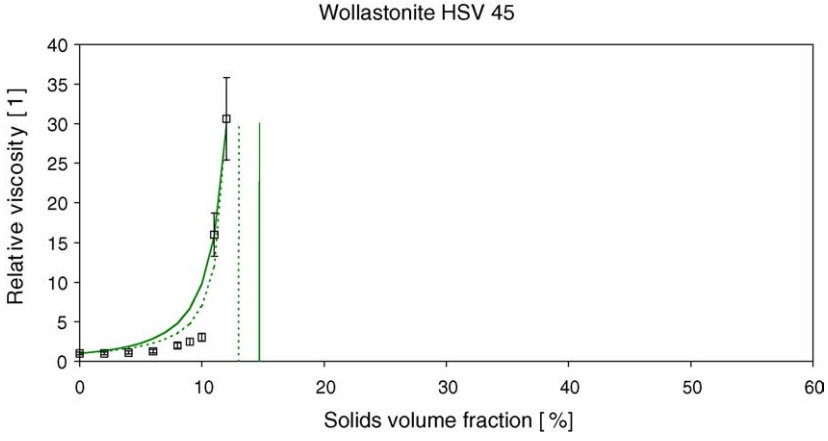

Fig. 3. Concentration dependence of the relative viscosity of suspensions with wollastonite HSV 45; measured data (empty squares), Krieger fit (dashed line), Maron–Pierce fit (full line); the corresponding critical volume fractions ϕ_c obtained by fitting are indicated as vertical asymptotics.

Table 8
Fit parameters ϕ_c and $[\eta]$ (and correlation coefficients C) for the concentration dependence of the relative viscosity of suspensions with different materials obtained with the Krieger relation

Material	ϕ_c (%)	$[\eta]$	C
Corn starch	76.0	4.72	0.994
Wheat starch	61.3	4.77	0.999
Average of both starch types	53.1	4.44	0.999
WM 45	36.3	4.70	0.992
HSV 45	13.0	10.2	0.975

Table 9
Fit parameters ϕ_c, estimates for the intrinsic viscosity $[\eta]_{est}$ and correlation coefficients C for the concentration dependence of the relative viscosity of suspensions with different materials obtained with the Maron–Pierce relation

Material	ϕ_c (%)	$[\eta]_{est}$	C
Corn starch	48.5	4.12	0.992
Wheat starch	47.7	4.19	0.997
Average of both starch types	47.9	4.18	0.999
WM 45	40.1	4.99	0.991
HSV 45	14.7	13.6	0.952

relation (Eq. (13)) and the Maron–Pierce relation (Eq. (14)), respectively. Mere visual inspection shows (and the correlation coefficients confirm) that the fits are excellent for starch and WM 45 suspensions, but relatively bad for HSV 45 suspensions, which is related to the high uncertainty of the values for 11 and 12 vol.% HSV 45 suspensions. Notwithstanding these minor details, however, it is evident that all experimentally determined intrinsic viscosity values are significantly higher than the theoretically predicted ones. In particular, the measured intrinsic viscosity of starch suspensions is almost the same as that of the low-aspect-ratio wollastonite WM 45. This might be a consequence of the fact that in real systems attractive interactions of electrostatic origin (causing particle agglomeration in suspensions) cannot be excluded to the necessary degree. It is clear that, in order to obtain the correct value of intrinsic viscosity in the dilute limit, the effective viscosities at higher concentrations (non-dilute range) must be minimized. In principle, this can be achieved by optimal deflocculation and stabilization of the suspension with the help of an appropriate dispersant. In our case, however, the situation is complicated by the presence of the organic component (saccharose), which makes possible cross-interactions hard to predict. Apart from interaction effects, which cause the measured intrinsic viscosities to be too high, it may also argued that the predicted intrinsic viscosities are too low because of the fact that the aspect ratio used for prediction purposes here is only an average aspect ratio and it is well thinkable that the actual intrinsic viscosity is determined mainly by the highest aspect ratios occurring in the system. Interestingly, the intrinsic viscosity values experimentally determined in this work for starch and the low-aspect-ratio wollastonite WM 45 (range 4.2–5.0) are remarkably close to the intrinsic viscosity value 4.5 recommended by the Bačinskij formula (Eq. (6)). This finding seems to be in agreement with long-term experimental experience of other authors.[10,11]

Similar conclusions can be drawn with respect to the critical volume fractions determined in this work. While for systems with isometric particles (starch suspensions), the critical volume fraction determined is approximately 53% (according to the Krieger fit) or 48% (according to the Maron–Pierce fit), in satisfactory agreement with the prediction via the empirical formula of Kitano et al. (Eq. (15)), ϕ_c values for the wollastonite suspensions are quite different from Kitano's predictions (cf. Fig. 4). Again, this is indicative of interaction (agglomeration) and, possibly, an increased influence of high-aspect-ratio particles in the system. By linear fitting the values (Maron–Pierce fit parameters) in Fig. 4, we obtain a Kitano-type expression with the following numerical coefficients

$$\phi_c = 0.51 - 0.0223\bar{R}. \tag{36}$$

Note that, compared to Eq. (15), especially the slope of the regression line is increased, i.e. in the presence of interactions

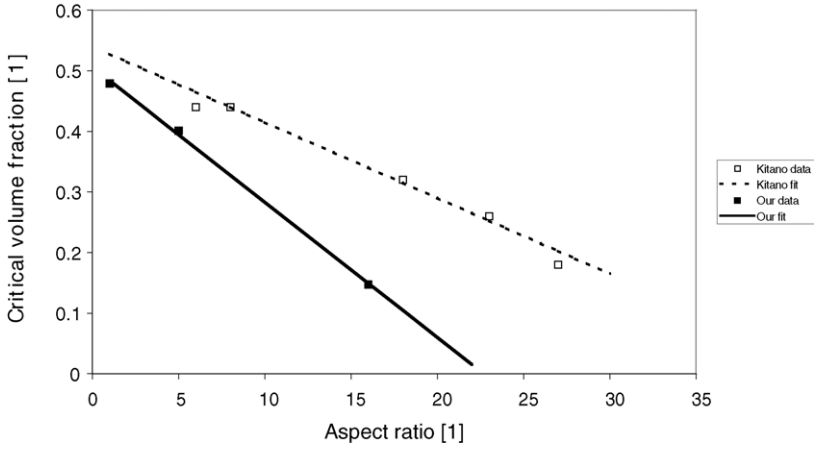

Fig. 4. Dependence of the critical volume fraction ϕ_c (obtained by fitting with the Maron–Pierce relation) on the average particle aspect ratio R; filled squares and full line are data and linear regression line, respectively, of this work; empty squares and dashed line are data and linear regression line, respectively, of Kitano et al.[22]

the critical volume fraction (at which blocking of the flowablility occurs) is much lower for particles with a comparable degree of anisometry.

5. Conclusion

This paper is intended to serve as a guideline for future experimental research on the rheology of fiber suspensions. In particular, we have given a very simple relation (Eq. (35)) for the dependence of the intrinsic viscosity on aspect ratio, which approximates the highly sophisticated Brenner relation (17) for many practical situations with sufficient precision. This approximate relation, formally the "non-Brownian" counterpart of the widely used Kuhn–Kuhn relation (31) for low-aspect-ratio Brownian particles, might be appealing to other investigators and is to enable easy comparison of theoretical predictions and experimental findings.

For the special case of wollastonite suspensions, the findings of this work clearly demonstrate that it is not possible to predict the intrinsic viscosity of these suspensions via the theoretically sound and well-founded Brenner formula (17) or its practical short-hand version (35). Consequently, even in the dilute limit the relative viscosity cannot be predicted by simply inserting Brenner's value of $[\eta]$ into the Jeffery–Einstein relation (4). The probable reasons (particle interactions and non-unique aspect ratio in real systems) have been discussed. When a rough estimate is needed for the relative viscosity of a suspension with low-aspect-ratio particles (average aspect ratio $\overline{R} < 5$, say) the Bačinskij relation (6), in other words Bačinskij's intrinsic viscosity value of $[\eta] = 4.5$, can be used. In practice, knowledge of the intrinsic viscosity alone should be sufficient to predict relative viscosities of suspensions containing low-aspect-ratio particles up to solids volume fractions of approximately 10% with satisfactory precision. For suspensions with high-aspect-ratio particles (average aspect ratio $\overline{R} > 10$, say), however, the intrinsic viscosity cannot be predicted. In this case, as well as for higher concentrations of low-aspect-ratio particles, the Maron–Pierce relation (14), in connection with a Kitano-type relation (Eqs. (15) or (36)), is the only alternative for roughly predicting relative suspension viscosities. Based on the findings of this work on wollastonite systems, we recommend Eq. (36), with the average aspect ratio $\overline{R}$ (arithmetic mean) for polydisperse short-fiber suspensions.

Acknowledgements

This work was part of the bilateral project "Size and shape characterization of particles in ceramic science and technology", supported by the Czech Ministry of Education, Youth and Sports and the German Bundesministerium für Forschung und Technik (Grant No. CZE 01/012) and the research programme "Preparation and properties of advanced materials—modelling, characterization, technology", supported by the Czech Ministry of Education, Youth and Sports (Grant No. MSM 223100002). It is based on fundamental research performed by W.P. within the project "Mechanics and thermomechanics of disperse systems, porous materials and composites", supported by the Grant Agency of the Czech Republic (Grant No. 106/00/D086). The support is gratefully acknowledged.

References

1. Anthony, J. W., Bideaux, R. A., Bladh, K. W. and Nichols, M. C., *Handbook of Mineralogy: Silica, Silicates (Part 2), Vol II*. Mineral Data Publishing, Tucson, Arizona, 1995, p. 879.
2. JCPDS, *Data sheets 84-0654 and 84-0655 (PCPDFWIN v. 2.3)*. International Centre for Diffraction Data (ICDD), 2002.
3. Torquato, S., *Random Heterogeneous Materials*. Springer, New York, 2002, pp. 1–58.
4. Pabst, W., Fundamental considerations on suspension rheology. *Ceram. Silik.*, 2004, **48**, 6–13.
5. Einstein, A., Eine neue Bestimmung der Moleküldimensionen. *Ann. Phys.*, 1906, **19**, 289–306;
   Einstein, A., A new determination of molecular dimensions. In *Investigations on the Theory of the Brownian Movement*, ed. R. Fürth. Dover, New York, 1956.
6. Jeffery, G. B., The motion of ellipsoidal particles immersed in a viscous fluid. *Proc. R. Soc. Lond. A*, 1922, **102**, 161–179.
7. Happel, J., *J. Appl. Phys.*, 1957, **28**, 1288.
8. Happel, J. and Brenner, H., The viscosity of particulate systems. *Low Reynolds Number Hydrodynamics*. Martinus Nijhoff, The Hague, 1983, pp. 431–473.
9. Kasatkin, A. G., *Základní pochody a přístroje chemické technologie [Basic Processes and Equipment of Chemical Technology], Vol 1*. Technicko-vědecké nakladatelství, Prague, 1952, pp. 32 and 142 [in Czech].
10. Nývlt, J., Sedimentace v suspenzích [Sedimentation in suspensions]. *Chemický průmysl*, 1962, **12**, 440–443 [in Czech].
11. Nývlt, J., Viskozita suspenzí [Viscosity of suspensions]. *Chem. Listy*, 2000, **94**, 45–47 [in Czech].
12. Brenner, H., Rheology of a dilute suspension of axisymmetric Brownian particles. *Int. J. Multiphase Flow*, 1974, **1**, 195–341.
13. Zirnsak, M. A., Hur, D. U. and Boger, D. V., Normal stresses in fibre suspensions. *J. Non-Newtonian Fluid Mech.*, 1994, **54**, 153–193.
14. Petrie, C. J. S., The rheology of fibre suspensions. *J. Non-Newtonian Fluid Mech.*, 1999, **87**, 367–402.
15. Petrich, M. P., Koch, D. L. and Cohen, C., An experimental determination of the stress–microstructure relationship in semi-concentrated fiber suspensions. *J. Non-Newtonian Fluid Mech.*, 2000, **95**, 101–133.
16. Pabst, W. and Gregorová, E., Rheology of platelet and fiber suspensions. In *Advances in Science and Technology (Proceedings of the 10th International Ceramics Congress CIMTEC, Part A), Vol 30*, ed. P. Vincenzini. Techna, Faenza, 2003, pp. 609–616.
17. Pabst, W., Kuneš, K., Havrda, J. and Gregorová, E., A note on particle size analysis of kaolins and clays. *J. Eur. Ceram. Soc.*, 2000, **20**, 1429–1437.
18. Pabst, W., Kuneš, K., Gregorová, E. and Havrda, J., Extraction of shape information from particle size measurements. *Br. Ceram. Trans.*, 2001, **100**, 106–109.
19. Pabst, W, Mikač, J., Gregorová, E. and Havrda, J., An estimate of orientation effects on the results of size distribution measurements for oblate particles. *Ceram. Silik.*, 2002, **46**, 41–48.
20. Lehmann, M., *Korngrössen- und Kornformcharakterisierung an Kaolinen, Ein Vergleich von Laserbeugungs- und Sedimentationsmethoden*. M.Sc. thesis, Universität Tübingen, 2003.

21. Lehmann, M., Berthold, C., Pabst, W., Gregorová, E. and Nickel, K. G., Particle size and shape characterization of kaolins—comparison of settling methods and laser diffraction. *Key Eng. Mater.*, 2004, **264–268**, 1387–1390.
22. Kitano, T., Kataoka, T. and Shirota, T., An empirical equation of the relative viscosity of polymer melts filled with various inorganic fillers. *Rheol. Acta*, 1981, **20**, 207–209.
23. Pabst, W., Berthold, C. and Gregorová, E., Size and shape characterization of polydisperse short-fiber systems. *J. Eur. Ceram. Soc.*, submitted for publication.
24. Doi, M. and Edwards, S. F., *J. Chem. Soc. Faraday Trans. II*, 1978, **74**, 560–570.
25. Doi, M. and Edwards, S. F., Semidilute and concentrated solutions of rigid rodlike polymers. *The Theory of Polymer Dynamics*. Clarendon Press, Oxford, 1986, pp. 324–380.
26. Larson, R. G., Particulate suspensions. *The Structure and Rheology of Complex Fluids*. Oxford University Press, New York, 1999, pp. 263–323.
27. Mori, Y., Ookubo, N., Hayakawa, R. and Wada, Y., *J. Polym. Sci.*, 1982, **20**, 2111.
28. Aste, T. and Weaire, D., *The Pursuit of Perfect Packing*. Institute of Physics Publishing, Bristol, 2000, pp. 20–24.
29. Zallen, R., *The Physics of Amorphous Solids*. Wiley, New York, 1983, pp. 49–59.
30. Rintoul, M. D. and Torquato, S., Computer simulations of dense hard-sphere systems. *J. Chem. Phys.*, 1996, **105**, 9258–9265.
31. Krieger, I. M., Rheology of monodisperse latices. *Adv. Colloid Interface Sci.*, 1972, **3**, 111–136.
32. Maron, S. H. and Pierce, P. E. J., *Colloid Sci.*, 1956, **11**, 80.
33. Huilgol, R. R. and Phan-Thien, N., *Fluid Mechanics of Viscoelasticity*. Elsevier, Amsterdam, 1997, pp. 239–270.
34. Phan-Thien, N. and Pham, D. C., Differential multiphase models for polydispersed spheroidal inclusions: thermal conductivity and effective viscosity. *Int. J. Eng. Sci.*, 2000, **38**, 73–88.
35. Chen, C.-H. and Cheng, C.-H., Micromechanics and apparent viscosities of non-Newtonian fluid suspensions. *Mech. Mater.*, 1998, **27**, 177–185.
36. Brenner, H., Dissipation of energy due to solid particles suspended in a viscous liquid. *Phys. Fluids*, 1958, **1**, 338–346.
37. Brenner, H., Coupling between the translational and rotational Brownian motions of rigid particles of arbitrary shape. Part II. General theory. *J. Colloid Interface Sci.*, 1967, **23**, 407–436.
38. Kuhn, W. and Kuhn, H., Die Abhängigkeit der Viskosität vom Strömungsgefälle bei hochverdünnten Suspensionen und Lösungen. *Helv. Chim. Acta*, 1945, **28**, 97–127.
39. Hinch, E. J. and Leal, L. G., The effect of Brownian motion on the rheological properties of a suspension of non-spherical particles. *J. Fluid Mech.*, 1972, **52**, 683–712.
40. Scheraga, H. A., Non-Newtonian viscosity of solutions of ellipsoidal particles. *J. Chem. Phys.*, 1955, **23**, 1526–1532.
41. Berthold, C., Klein, R., Lühmann, J. and Nickel, K. G., Characterization of fibres and fibre collectives with common laser diffractometers. *Part. Part. Syst. Charact.*, 2000, **17**, 113–116.
42. Bretschneider, R., Bohačenko, I., Kadlec, P., Kopřiva, B. and Svoboda, A., *Cukrovarnické tabulky [Tables for Sugar Production]*. SNTL, Prague, 1975, pp. 98–196 [in Czech].